Dalton
Transactions

RSC Publishing

PAPER

View Article Online
View Journal | View Issue

Cite this: *Dalton Trans.*, 2013, **42**, 13210

A novel thermally stable hydroperoxo–copper(II) complex in a Cu(N_2O_2) chromophore of a potential N_4O_2 donor Schiff base ligand: synthesis, structure and catalytic studies†

Surajit Biswas, Arpan Dutta, Mainak Debnath, Malay Dolai, Kalyan K. Das and Mahammad Ali*

Received 28th May 2013,
Accepted 18th June 2013

DOI: 10.1039/c3dt51359a

www.rsc.org/dalton

The generation and study of metal–hydroperoxo/metal–peroxo (LCu^{II}–OOH or LCu^{II}–$OO^{\cdot}$) complexes is a fascinating area of research of many chemical and biochemical researchers, because of their involvement as active intermediates in many biological and industrial catalytic oxidation processes. For this purpose we have designed a bulky hexa-coordinating ligand with potential N_4O_2 donor atoms which could provide an opportunity to synthesize a mononuclear Cu(II) complex with an aim to utilize it in the catalytic oxidation of aromatic hydrocarbons by an environmentally benign oxidant, H_2O_2. The Cu(II) complex (**1**) was structurally characterized and found to have square-planar geometry with the two pyrazolyl groups remaining in dangling mode. A novel mononuclear complex [Et_3NH][LCu^{II}–OOH] (**2**) was found to form in the reaction between **1** and H_2O_2 in the presence of Et_3N. The presence of this dangling groups favours the stability of hydroperoxo species, $[LCu–OOH]^-$ (**2**) through H-bonding with the coordinated phenoxo oxygen atom, which was confirmed by ESI-MS^+ and MS^- (*m*/*z*) mass analysis and DFT calculations. This complex was found to be thermally stable at room temperature [$k_d = (5.67 \pm 0.03) \times 10^{-5}\ s^{-1}$ at 25 °C] and may be due to the formation of O–O–H⋯O(phenoxo) H-bonding as delineated by the DFT calculations. Complex **1** was found to be an efficient catalyst for the oxidation of aromatic hydrocarbons to the corresponding aldehyde and alcohol in 2 : 1 mole ratio with TON ~300.

Introduction

The generation and study of metal–hydroperoxo (LCu^{II}–OOH) and metal–peroxo (LCu^{II}–$OO^{\cdot}$) complexes is a fascinating area of interest for many chemical and biochemical researchers, because of their involvement as active intermediates in many biologically and industrially important catalytic oxidation processes.[1–3] The characterization of these thermally unstable hydroperoxo intermediates is very difficult due to their very short lifetimes. The mononuclear hydroperoxo[4] and superoxo[5–8]–Cu^{II} species, formed by the reaction between LCu^I and O_2, have been proposed as reactive intermediates in the aliphatic hydroxylation of substrates by many enzymes such as peptidylglycine α-amidating monooxygenase (PAM) and dopamine β-monooxygenase (DβM) and have vigorously been synthesized and investigated as model complexes.[9,10] The formation of LCu^{II}–OOH species through the abstraction of an H-atom from a substrate by LCu^{II}–$OO^{\cdot}$ species has been supported by DFT calculations.[8]

Mononuclear Cu^{II}–hydroperoxo complexes[9,11–21] are also believed to be formed by the addition of H_2O_2/base to a precursor copper(II) complex. Though there are numerous reports on LCu–OOH species, most of these are limited to $Cu^{I/II}$-complexes of tripodal N_4 donor ligands, which were characterized only in solution phase at very low temperature (~liquid nitrogen temperature) by spectroscopic means. Masuda and coworkers[9] were the only ones who have been able to obtain an X-ray crystal structure of a LCu–OOH complex employing a tripodal tetradentate ligand with additional (CO–NH) groups as H-donor to the coordinated oxygen atom of –OOH to stabilize the species in solid state. Thus, the chemistry of L–Cu^{II}–($O_2^{\cdot -}$)/L–Cu–OOH species has mostly been limited to tripodal tetradentate N_4 donor ligands such as tris(2-pyridylmethyl)amine (TMPA) and analogues or derivatives of tris(2-aminoethyl)amine, tren[22–28] and extensively studied only in solution.

Department of Chemistry, Jadavpur University, Kolkata 700 032, India. E-mail: mali@chemistry.jdvu.ac.in

†Electronic supplementary information (ESI) available. CCDC 905948. For ESI and crystallographic data in CIF or other electronic format see DOI: 10.1039/c3dt51359a

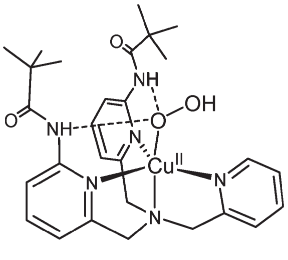

Scheme 1

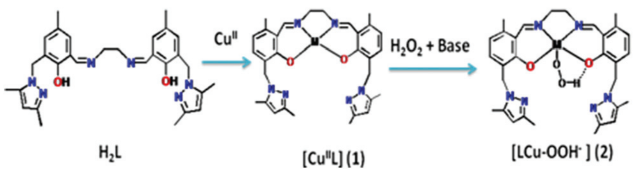

Scheme 2

The only report by Masuda *et al.* gives us an idea to design a ligand in bulky environment with phenoxo oxygen atoms which simultaneously coordinates to the metal center and provides an opportunity to form an H-bond with the H-atom of a coordinated –OOH group thereby stabilizing the otherwise unstable LCu–OOH species (Scheme 1). In this research endeavour, we have been successful in designing such a ligand (H_2L) with mixed donor atoms (N_4O_2) and found to stabilize LCu^{II}–OOH through H-bonding (Scheme 2).

Soil and sediment bacteria like *Pseudomonas putida* is the most extensively characterized catabolic plasmid that encodes enzymes for the mineralization of toluene, *m*- and *p*-xylenes, *m*-ethyltoluene and 1,3,4-trimethylbenzene[29,30] in which the methyl group at carbon 1 in the aromatic ring is oxidized to yield the corresponding carboxylic acid, which is subsequently oxidized in a number of steps to give pyruvate and aldehydes as the final products.[31] Chemical catalytic oxidation of hydrocarbons to the corresponding alcohol, phenol, carbonyl or carboxylic acid is an extremely fascinating area of research, owing to their extensive applications as precursors in a wide variety of organic synthesis in the laboratory as well as in industry.[32–34] Recently it has been observed that many transition-metal complexes, in combination with various oxidizing agents, can catalyze the oxidation of a variety of hydrocarbons including lower alkanes.[35]

Monomeric copper–Schiff base complexes are important in modelling metallobioenzymes[36–39] as well as from the industrial perspective[40] and a great amount of research attention has been paid to understand the reactivity of metalloradicals involved in free-radical catalysis such as GOase[41–43] along with some industrially important catalytic reactions such as oxidative coupling polymerization of phenol derivatives,[44] oxidation of hydrocarbons[45–48] *etc.*, which provide an environmentally benign method. Though, copper–Schiff base compounds have been widely used as catalysts in oxidation of hydrocarbons, yields and TON (turn over number) obtained are not very remarkable so far.[45–48] Recent reports have described the reactivity of copper–peroxo species with hydrocarbons to produce the corresponding alcohols and acids.[45–48]

All these lead us to design and synthesize a molecule which could have potential ability to catalyze hydrocarbon oxidation. For this purpose we have designed a bulky hexa-coordinating flexidentate ligand with potential N_4O_2 donor atoms which could provide an opportunity to synthesize mono- as well as multinuclear complexes. In the case of mononuclear copper(II) complexes with dangling pyrazole groups there is ample possibility to obtain stable hydroperoxo-species due to H-bonding between the –OOH group and pyrazole N-atoms as delineated by Masuda.[9] Though there are numerous reports on structure–reactivity relationship of LCu–OOH intermediates that are transiently generated in the medium and mostly characterized by spectroscopic methods, these are based on tetradentate N_4 donor ligands. To the best of our knowledge this constitutes the first report on a stable $LCu–OOH^-$ species of a tetradentate N_2O_2 Schiff base ligand that can be stabilized thermally. We report here the synthesis and crystal structure of a mononuclear copper(II) complex (**1**) and catalytic oxidation of aromatic hydrocarbons by H_2O_2. We have selected hydrogen peroxide as the oxidant of choice due to its ability to function under ambient mild conditions as well as its low cost.

Experimental section

Materials and reagents

2-(Hydroxymethyl)-6-carbaldehyde-4-methylphenol and 2-(chloromethyl)-6-carbaldehyde-4-methylphenol were prepared by reported methods.[49] All reagents and solvents are commercially available. THF was dried using sodium metal and benzophenone and other solvents were used without further purification.

Physical measurements

Elemental analyses were carried out using a Perkin-Elmer 240 elemental analyzer. ^1H NMR were recorded in $CDCl_3$ on a Bruker 300 MHz NMR Spectrophotometer using tetramethylsilane ($\delta = 0$) as an internal standard. Electronic spectra were recorded on Agilent-8453 diode array UV-Vis spectrophotometer. ESR spectra were recorded on JOEL JES-FA 200 ESR spectrometer. ESI-MS$^+$ and MS$^-$ (*m*/*z*) were recorded on Waters Qtof Micro YA263 mass spectrometer.

Synthesis of proligand 2-formyl-4-methyl-6-[3,5-dimethylpyrazole]phenol

2-Chloromethyl-6-carbaldehyde-4-methylphenol (1.52 g, 8.2 mmol) was dissolved in 15 ml dry THF in a round bottom flask. 0.7883 g (8.2 mmol) 3,5-dimethylpyrazole and 1.659 g (16.4 mmol) triethylamine (Et_3N) were dissolved in 5–10 ml dry THF separately. Then the latter solution was added to the previous one and this mixture was further added dropwise to the 2-chloromethyl-6-carbaldehyde-4-methylphenol solution. An instant precipitation of Et_3NHCl was observed and the colour of the solution turned bright yellow. After 24 h of stirring the precipitate was filtered off. The filtrate was then concentrated by removing THF under reduced pressure. After a few days under vacuum a light yellow solid was obtained. Yield ~70% ^{1}H NMR (in $CDCl_3$, 300 MHz, ppm): δ 2.23–2.28 (9 H, m, –$ArCH_3$), 5.27 (2H, s, –CH_2), 7.09 (1H, s, –ArH), 7.27 (1H, s, –ArH), 7.28 (1H, s, –ArH), 9.88 (1H, s, –CHO), 11.23 (1H, br s, –ArOH).

Syntheses of [Cu^{II}(L)] (1)

A mixture of 2-formyl-4-methyl-6-(3,5-dimethylpyrazole)phenol (0.244 g, 1 mmol) and ethylenediamine (0.03 g, 0.5 mmol) in 30 ml methanol was refluxed for 45 min. After cooling to room temperature copper perchlorate hexahydrate (0.185 g, 0.5 mmol) was added and refluxing was continued for a further 90 min. The yellow coloured solution turned brown. It was filtered and the filtrate was kept in a rack. Slow evaporation of methanol gave rod-shaped brown crystals suitable for X-ray studies. Elemental analysis: Calc. for $C_{30}H_{34}N_6O_2Cu$ (M = 574.18): C, 62.70; H, 5.92; N, 14.63; Found: C, 62.34; H, 6.09; N, 14.46%.

Single-crystal X-ray diffraction studies

Intensity data for complex **1** was collected at 293(2) K on a Bruker SMART APEX-II CCD diffractometer using graphite-monochromated Mo-K$_\alpha$ radiation (λ = 0.71073 Å and the ω–2θ scan mode in the range $2.3 < 2\theta < 27.5°$). No decomposition of the crystal occurred during the data collection. The intensities were corrected for Lorentz and polarization effects and for absorption using the ψ-scan method. The cell parameters were refined from all strong reflections. The data reductions were carried out using the CrysAlis RED (Oxford Diffraction, UK) program, and analytical absorption corrections were applied. The structure was determined by direct methods using SHELXS-97[50] and refined anisotropically on F^2 using the full-matrix least-squares procedure of SHELXL-97.[50] The crystallographic data for **1** are given in Table 1.

Table 1 Details of crystallographic data collection and refinements

Formula	$C_{30}H_{34}N_6O_2Cu$
M_r	574.18
Crystal system	Monoclinic
Space group	$C2/c$ (no. 15)
a/Å	21.53600
b/Å	9.92000
c/Å	13.03300
β/°	108.9800
V/Å^3	2632.954
Z	4
D_c/g cm^{-3}	1.448
μ(Mo-Kα)/mm	0.870
F(000)	1204
T/K	293
λ/Å	0.71073
$\theta_{min,max}$/°	2.3, 27.5
Dataset, hkl	−27, 27; −12, 12; −16, 16
Total, unique data, R_{int}	5843, 3028, 0.013
Observed data [$I > 2.0\sigma(I)$]	2734
N_{ref}, N_{par}	3028, 245
R, wR_2, S	0.0310, 0.1185, 1.09

DFT calculations

The calculations were started with molecular structures of [Cu(L)] (**1**) obtained from the single-crystal X-ray diffraction and also on its hydroperoxo derivative [LCu–OOH]$^-$ (**2**) with peroxide ligated axially to the metal center. Their ground-state geometries were fully optimized by DFT calculations using the Gaussian 03 program[51] with the Becke three-parameter hybrid functional (B3LYP).[52,53] The LanL2DZ[54] valence and effective core potential functions were used for all atoms including copper. These basis functions were augmented with additional polarization functions of the exponents: Cu (ζ_f = 0.8), C (ζ_d = 0.8), N (ζ_d = 0.8), O (ζ_d = 0.8). The nature of all stationary points was confirmed by performing a normal-mode analysis.

Experimental set up for catalytic oxidation

A mixture of complex **1** (the catalyst) (32 mg, 0.0555 mmol) and the substrate (hydrocarbon) (20 mmol) was dissolved in 10 ml dry MeCN solvent and the resulting solution was taken into a 50 ml capacity two-neck round bottom flask of which one neck was closed with a rubber septum and the other was fitted with a condenser. To the above solution was then added 2 ml of 30% H_2O_2 and the resulting solution immediately turned brownish green. The solution was then heated on an oil-bath to reflux for 24 h. An aliquot (0.10 ml) of the reaction solution was withdrawn with the help of long needle syringe at regular time intervals (Table 3) and was subjected to multiple ether extraction and 1 µL of concentrated ether extract was then injected into the GC port with the help of a 10 µL syringe. The retention times of the peaks were compared with those of commercial standards.

Structural descriptions

Single-crystal X-ray structural analysis reveals a square-planar Cu(II)–Schiff-base complex **1** (Fig. 1) where Cu1 is found to be tetra-coordinated. The two ethylenediamine N atoms (N1 and N2) and two phenoxo O atoms (O2 and O3) satisfy four

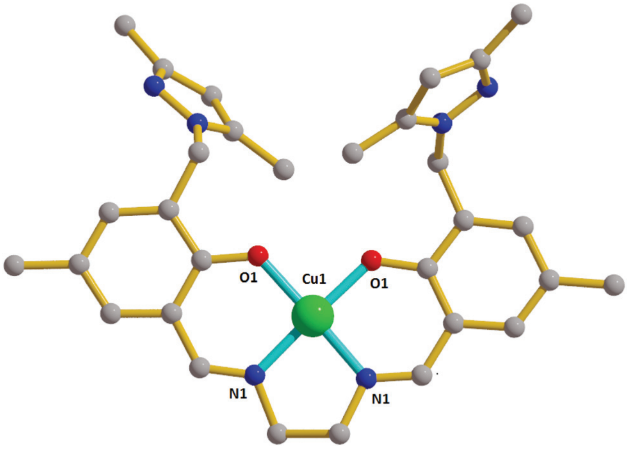

Fig. 1 Molecular view with atom numbering scheme of **1**. All H-atoms are omitted for clarity. Symmetry code: (A) x, y, z; (B) $-x, y, 1/2 - z$; (C) $1/2 + x, 1/2 + y, z$; (D) $1/2 - x, 1/2 + y, 1/2 - z$; (E) $-x, -y, -z$; (F) $x, -y, 1/2 + z$; (G) $1/2 - x, 1/2 - y, -z$; (H) $1/2 + x, 1/2 - y, 1/2 + z$.

Table 2 Selected bond lengths (Å) and bond angles (°) for complex **1**; values in parentheses are for the DFT optimized structure of **1**

Bond lengths/Å		Bond angles/°	
Cu1–O1	1.8985(12) [1.930]	O1–Cu1–N1	93.38(5) [92.0]
Cu1–N1	1.9406(14) [1.987]	O1–Cu1O1a	88.96(5) [93.3]
Cu1–O1a	1.8985(12) [1.935]	O1–Cu1–N1a	175.22(5) [92.0]
Cu1–N1a	1.9406(14) [1.987]	O1a–Cu1–N1	175.22(5) [171.1]
		N1–Cu1–N1a	84.61(6) [83.6]
		O1a–Cu1–N1a	93.38(6) [92.0]

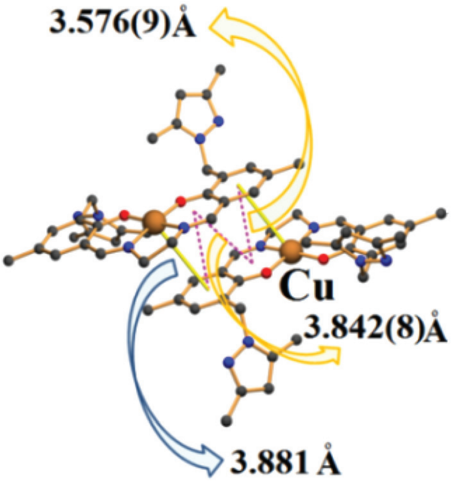

Fig. 2 *Chelate ring–π(phenyl)*, *chelate ring–chelate ring* and *Cu–π(phenyl)* interactions in complex **1**.

coordination sites. Cu1–N (ethylenediamine) and Cu1–O (phenoxo) bond distances are typical of square-planar Cu complexes[55] (Table 2).

Interesting π-stacking interactions govern the supramolecular assembly of the mononuclear units in **1** (Fig. 2). In complex **1** there are *chelate ring–π(phenyl)* and *chelate ring–chelate ring* π-stacking interactions and also the *Cu–π(phenyl)* interactions that stabilize the dimer of two mononuclear units. Also an additional CH–π interaction comes into play between the methyl group attached to the phenyl ring and the six-membered chelate ring involving Cu in **1**.

The π-stacking interactions are self-complementary and successively join symmetry related mononuclear units along the crystallographic *c*-axis (Fig. 3). Simultaneously each mononuclear unit is also involved in CH–π interactions (Fig. S1†) in which the ethylene C–H group acts as a donor to the pyrazole ring of the symmetry related unit. This interaction propagates the supramolecular assembly along the crystallographic *b*-axis. Thus a 2D supramolecular sheet in the *bc*-plane is generated (Fig. 3) which is further stacked along the crystallographic *a*-axis (Fig. 4).

Copper(II)–hydroperoxo complex and its characterization

The copper(II)–hydroperoxo complex, $[Cu(L)(OOH)]^-$ (**2**), was prepared by adding 10 equivalents of H_2O_2 to a reaction solution containing **1** in the presence of 2 equivalents of

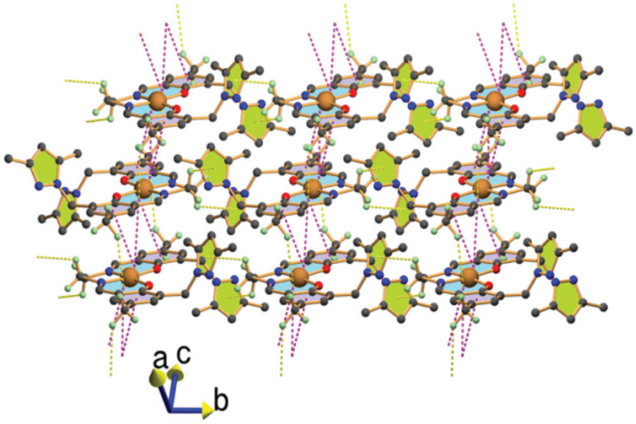

Fig. 3 The π-stacking (dotted lines in magenta color) and CH⋯π interaction (dotted lines in yellow color) leads to a supramolecular sheet in the *bc* plane for the Cu complex.

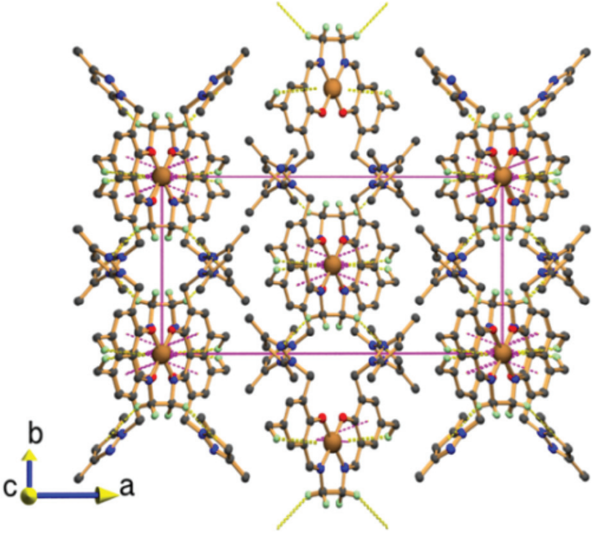

Fig. 4 The packing of supramolecular sheets along the crystallographic *a*-axis for the Cu complex.

triethylamine (TEA) in a solvent mixture of CH_3CN and CH_3OH (1 : 1) at 25 °C; the color of the solution changed from brown to brownish-green (Scheme 2). The UV-Vis spectrum of **2** shows an intense band at 374 nm ($\varepsilon = 2589\ M^{-1}\ cm^{-1}$) and a weak band at 572 ($\varepsilon = 234\ M^{-1}\ cm^{-1}$) (Fig. 5), which are similar to those of previously reported Cu^{II}–OOR complexes.[14,55–57] The former absorption peak has been assigned to a $HOO^- \rightarrow Cu^{II}$ ligand-to-metal charge-transfer transition (LMCT) and the latter band as d–d transition of the Cu^{II} ion in a square-pyramidal geometry. The corresponding bands of complex **1** appear at 360 nm ($\varepsilon = 2420\ M^{-1}\ cm^{-1}$) and 550 nm ($\varepsilon = 155\ M^{-1}\ cm^{-1}$). On addition of H_2O_2 in presence of a base there are red shifts by ~14 and ~22 nm for the absorption peaks at 360 and 550 nm, respectively of the parent complex **1** along with the increase in intensities. Though the complex [TEAH][Cu(L)(OOH)] was found to be stable in solution we could not isolate it in the solid state. The ESI-MS$^+$ of **1** in presence of

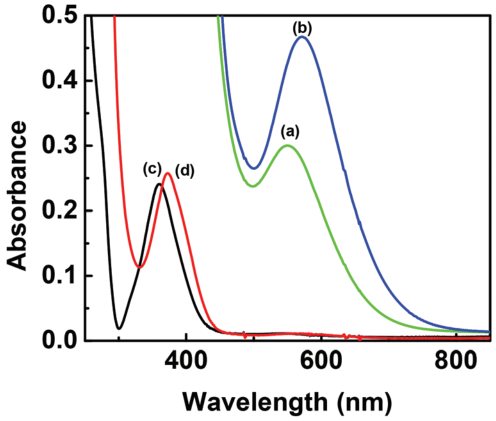

Fig. 5 Spectral change at room temperature for (a) **1** (2.0 mM); (b) **1** (2.0 mM) + H_2O_2 (50.0 mM) + NEt_3 (50.0 mM); (c) **1** (0.1 mM); (d) **1** (0.1 mM) + H_2O_2 (1.0 mM) + NEt_3 (1.0 mM).

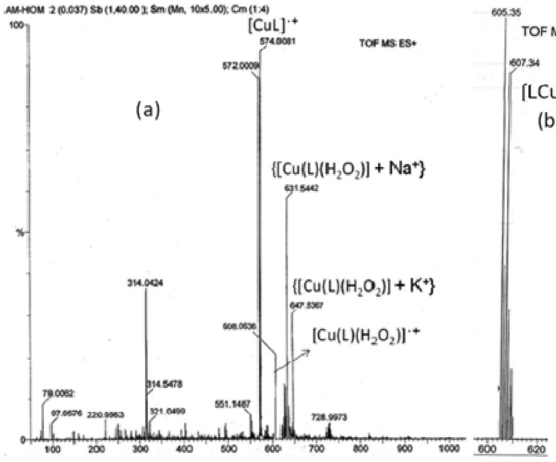

Fig. 6 (a) ESI-MS^+ of **1** in the presence of H_2O_2 and added HNO_3 and (b) ESI-MS^- (*m*/*z*) spectra for **1** in the presence of H_2O_2 and TEA.

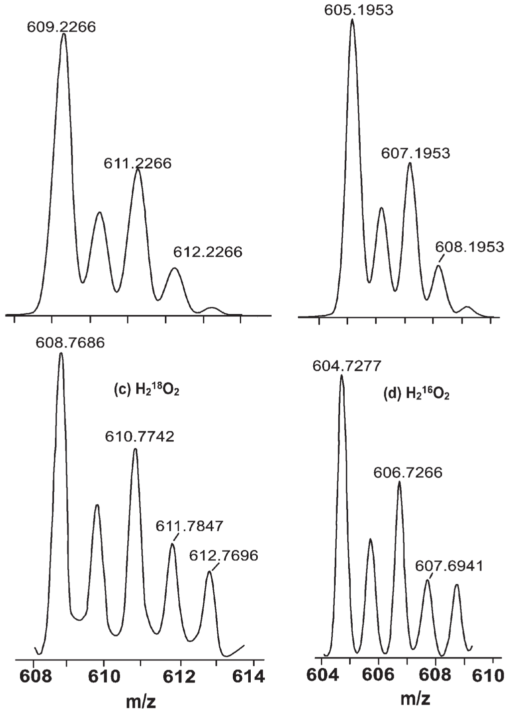

Fig. 7 ESI-MS^- spectra for **2**-$^{16}O_2$ (bottom left hand side) and **2**-$^{18}O_2$ (bottom right hand side) and their corresponding simulated spectra (top).

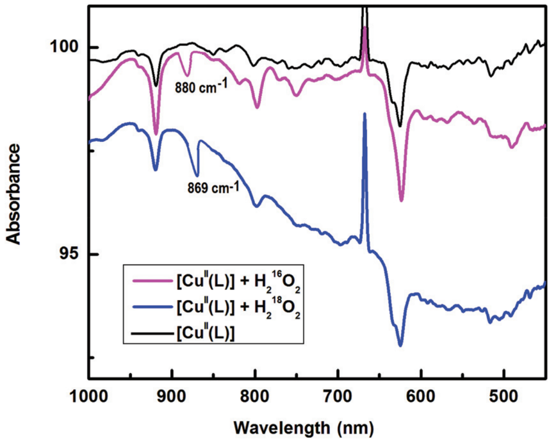

Fig. 8 IR spectra of complex **1** in MeCN (black) and also in presence of $H_2{}^{16}O_2$ (**2**-$^{16}O_2$) (magenta) and $H_2{}^{18}O_2$ (**2**-$^{18}O_2$) (blue).

H_2O_2 and HNO_3 (1 : 10) exhibits a prominent ion peak at 574 (Fig. 6a), whose mass corresponds to $[Cu(L)]^{•+}$ (calculated *m*/*z*, 574.18), characteristic of the parent complex. There are three other ion peaks at 608 ($[Cu(L)(HOOH)]^{•+}$); 631 ($[Cu(LH)(OOH)] + Na^+$) and 647 ($[Cu(LH)(OOH)] + K^+$) (Fig. 6a). The ESI-MS^- spectrum of **1** in MeCN in the presence of H_2O_2 and TEA appears at 607 (Fig. 6b) whose mass and isotope distribution pattern corresponds to $[Cu^{II}(L)(OOH)]^-$ (**2**-^{16}O).

When the reaction was carried out with isotopically labeled $H_2{}^{18}O_2$, a mass peak corresponding to $[Cu^{II}(L)(^{18}O^{18}OH)]^-$ (**2**-^{18}O) appeared at *m*/*z* of 611 (Fig. 7). The shift in four atomic mass units on substitution of ^{16}O with ^{18}O proves that **2** contains an O_2 unit. The ESI-MS^- (*m*/*z*) peaks in the ESI-MS spectrum indicate the absence of the formation of $[LCu(\mu\text{-}OH)_2CuL]^{2-}$ species in solution. So it could be concluded that $[LCu^{II}\text{–}OOH]^-$ is definitely formed in the solution. This is further proved by IR studies (Fig. 8) where a new band appears at 880 cm^{-1} corresponding to O–O stretching vibration which is very close to the DFT optimized value of 896 cm^{-1} (*vide infra*). When we treated complex **1** with $H_2{}^{18}O_2$ in presence of TEA the same band appears at 869 cm^{-1} indicating firmly the coordination of HOO^- to the Cu(II) center of the complex.

The stability of [LCu–OOH] (**2**) in MeCN was determined spectrophotometrically by following the decomposition of *in situ* formed species by reacting **1** (3.0×10^{-4} M) with H_2O_2 (3.0×10^{-3} M) in the presence of NEt_3 (3.90×10^{-3} M). The rate of decomposition was determined by initial rate method and found to be $k_d = (5.67 \pm 0.03) \times 10^{-5}\ s^{-1}$. This clearly points out that $[LCu\text{–}OOH]^-$ is fairly stable in MeCN.

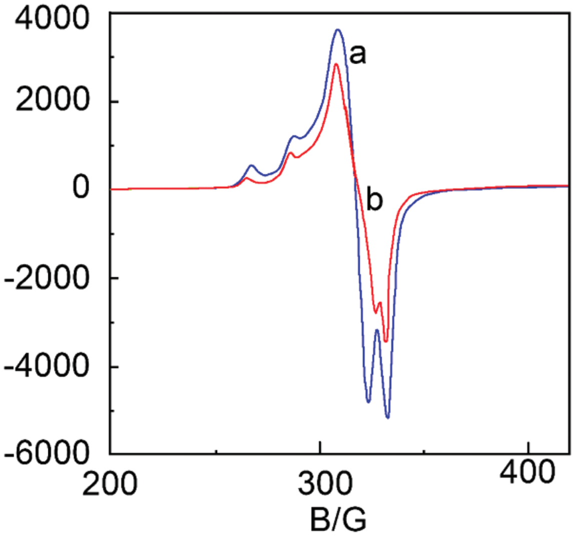

Fig. 9 X-Band EPR at 70 K: (a) **1** (0.5 mM in MeCN); (b) **1** (0.5 mM in MeCN) + 5.0 mM H_2O_2 + 5.0 mM NEt_3.

The ESR spectra of **1** and **2** are shown in Fig. 9. The spectrum of **1** ($g_{\|}$ = 2.264, $g_{\perp}$ = 2.12, $A_{\|}$ = 200 G) is clearly different from the spectrum of **2** ($g_{\|}$ = 2.566, $g_{\perp}$ = 2.38, $A_{\|}$ = 170 G). Thus shifts in g and A values clearly indicates a change in geometry on going from **1** to **2** *i.e.* –OOH definitely coordinates to the metal center axially and in solution both the complexes are roughly in square-pyramidal geometry.

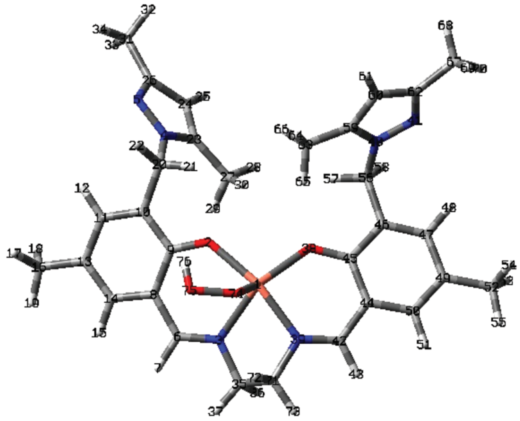

Fig. 10 DFT optimized geometry of **2**-OOH.

Table 3 Selected FT optimized bond lengths (Å) and bond angles (°) for complex **2**

Bond lengths/Å		Bond angles/°	
Cu1–O2	2.04	O2–Cu1–N3	85.2
Cu1–N3	2.28	O38–Cu1–ON39	88.0
Cu1–O38	2.06	N3–Cu1–N39	77.3
Cu1–N39	2.04	O2–Cu1–O38	98.5
Cu1–O74	1.97	O2–Cu1–N39	161.9
O74–O75	1.44	O38–Cu1–N3	126.6
O2···H76	2.26	Cu1–O7–O75	113.0

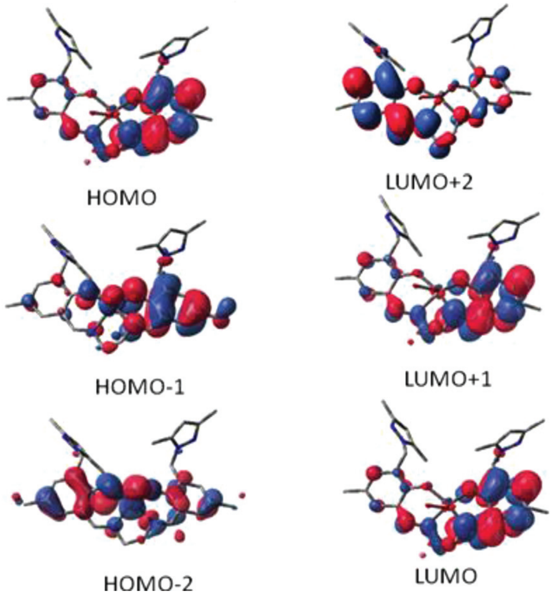

Fig. 11 HOMO and LUMO diagrams of [Cu(L)].

DFT optimized structure

Table 2 displays some important geometrical parameters optimized for the ground state. These gas-phase data are compared with those obtained from the X-ray diffraction studies. In the basal plane the Cu–O and Cu–N bond distances of the parent complex **1** and DFT optimized geometry of **1** differ only by 0.047 and 0.031 Å, respectively. The general agreement between these two sets of data is very good. We have also optimized the $[Cu(L)(OOH)]^-$ species **2**, where the –OOH group is attached to the copper centre axially, which is expected to be the reactive intermediate of the catalytic cycle in the oxidation of aliphatic and also aromatic hydrocarbons. Fig. 10 displays the optimized geometry of **2** and corresponding bond lengths and bond angles are listed in Table 3. MO diagrams for complexes **1** and **2** are depicted in Fig. 11 and 12, respectively. The HOMO–LUMO energy gaps appear to be 3.52 and 3.65 eV for complexes **1** and **2**, respectively. The differences in Cu–O and Cu–N bond lengths between **1** and **2** are 0.161 and 0.34 Å, respectively. The larger differences in bond lengths between **1** and **2** are quite logical, and are comparable to previous observations.[9] The Cu–peroxide geometry obtained is, as expected, of the end-on η^1-type with the coordinating atoms of the ligand in a square-pyramidal fashion with τ = 0.85, in agreement with the EPR spectroscopic results described above. The Cu–O74 (hydroperoxo) bond length is 1.97 Å and close to the value of 1.888 Å reported by Masuda and co-workers.[9] The Cu–O74–O75 angle of 113° is also in good agreement with the value reported by Masuda (114.5°). It is interesting to note that there is a strong O···H–O–O H-bonding interaction (O2···H76 = 2.27 Å) between phenoxo–O and peroxo H atoms which is shorter than the NH···O(OOH) bond distance (2.78 Å), as found by Masuda and co-workers, and believed to

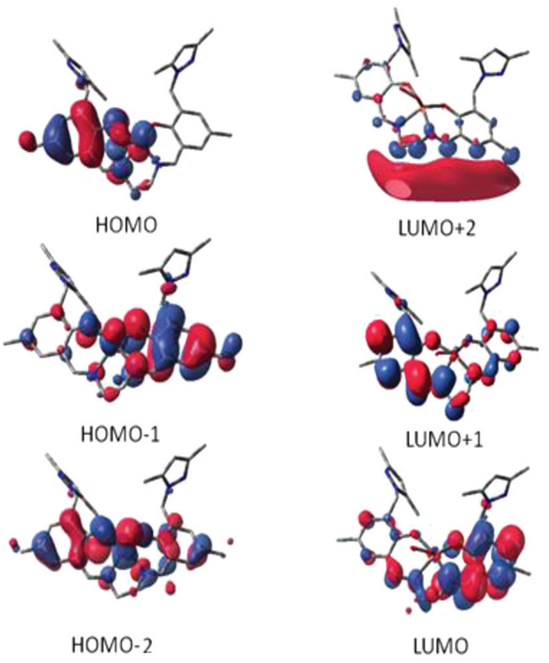

Fig. 12 HOMO and LUMO diagrams of $[Cu(L)–OOH]^-$.

be responsible for the stability of hydroperoxo species. The IR spectrum showed a prominent peak at ~879 cm^{-1} and matches reasonably well with the DFT optimized value (896 cm^{-1}) in the gas phase.

Probable mechanism of catalytic hydrocarbons oxidation

Complex **1** has been tested for the peroxidative oxidation of cyclohexane and toluene by H_2O_2 as oxidant, in a slightly acidic (HNO_3) medium under ambient conditions. A mixture of complex **1** (the catalyst) (0.0555 mmol), and the hydrocarbon substrate (20 mmol) was refluxed in 10 ml dry MeCN solvent in a 50 ml two-necked round bottom flask and the catalysis were initiated by adding 2 ml of 30% H_2O_2. Toluene and xylenes were oxidized to the corresponding alcohol and aldehyde. The yield was optimized by varying the relative proportion of hydrogen peroxide with respect to the catalyst, and also varying the reaction time. It has been evident from previous studies by other groups that the presence of nitric acid has a positive role in such catalytic reactions.[58–61] The added nitric acid has numerous roles in that (i) it increases the oxidation properties of the catalyst by increasing the unsaturation at the metal center (by protonation of the ligand); (ii) prevents decomposition of peroxide present in the reaction medium as oxidant; and (iii) enhances the stability of the peroxo intermediate formed in the reaction. The ratio $n(HNO_3)/n$(catalyst) has been optimized as 10 and all experiments were performed under this condition.

Table 4 Oxidation of toluene by complex **1** (0.055 mmol)

$n(H_2O_2)$/ n(catalyst **1**)	t/h	Yield (%) Benzyl alcohol	Yield (%) Benzaldehyde	Total conv. (%)	Sel. benzyl alcohol	TON
150	3	13	4	17	76.4	
	6	27	7	34	79.4	
	9	41	10	51	80.3	
	12	51	11	62	82.2	
	24	57	13	70	81.4	255
300	3	15	5	20	75.0	
	6	29	8	37	78.3	
	9	44	9	53	83.0	
	12	54	12	66	81.8	
	24	61	14	75	81.3	273
500	3	18	8	26	69.2	
	6	32	9	41	78.0	
	9	49	11	60	81.6	
	12	55	14	69	79.7	
	24	66	16	82	80.4	298

Table 5 Oxidation of *o*-xylene by complex **1** (0.055 mmol)

$n(H_2O_2)$/ n(catalyst **1**)	t/h	Yield (%) Alcohol	Yield (%) Aldehyde + acid	Total conv. (%)	Selectivity alcohol	TON
150	3	11	2	13	84.6	
	6	24	5	29	82.7	
	9	40	8	48	83.3	
	12	49	10	59	83.0	
	24	53	12	65	81.5	236
300	3	13	3	16	81.2	
	6	25	5	30	83.3	
	9	40	9	49	81.6	
	12	52	11	63	82.5	
	24	56	13	69	81.1	251
500	3	14	3	17	82.3	
	6	29	7	36	80.5	
	9	47	11	58	81.0	
	12	53	13	66	80.3	
	24	62	15	77	80.5	280

ESI MS^+ (m/z) mass spectra of complex **1** in the presence of nitric acid as well as in TEA and H_2O_2 showed the presence of copper–hydroperoxo species in the medium. The results of the oxidation of toluene, *o*-xylene and *p*-xylene are shown in Tables 4–6. It can be clearly seen from Tables 4–6 that complex **1** is a very efficient catalyst for the oxidation of toluene with 82% conversion (TON = 298) when the $n(H_2O_2)/n$(catalyst) ratio is 500, with a reaction time of 24 h. It has been observed for all the catalytic conversions that the yield increases with time. Catalytic conversions are also dependant on the amount of oxidant used. These results are comparable with the previously reported studies.[62] Fig. S2† shows the plot of the percentage yield of alcohol with reaction time. Simple copper salts, like $Cu(NO_3)_2$, under the same reaction conditions exhibit less than 4% conversion using the above mentioned substrates at $[n(H_2O_2)/n(\text{catalyst}) = 500]$. So it is evident that the presence of N and O donor ligands is quite relevant. The mechanism of the catalytic conversion is schematically given in Scheme 3. The LCu^{II} complex reacts with H_2O_2 to form the $L^HCu^{II}–OOH$ intermediate where one proton from HOOH is attached to a

Table 6 Oxidation of *p*-xylene by complex **1** (0.055 mmol)

$n(H_2O_2)$/ n(catalyst **1**)	t/h	Yield (%) Alcohol	Yield (%) Aldehyde + acid	Total conv. (%)	Selectivity alcohol	TON
150	3	10	4	14	71.4	
	6	22	5	27	81.4	
	9	38	8	46	82.6	
	12	48	12	60	80.0	
	24	55	15	70	78.6	255
300	3	13	3	16	81.2	
	6	27	6	33	81.8	
	9	42	11	53	79.2	
	12	54	13	67	80.6	
	24	60	15	75	80.0	273
500	3	14	5	19	73.6	
	6	33	8	41	80.5	
	9	47	12	59	79.6	
	12	57	13	70	81.4	
	24	59	19	79	74.7	287

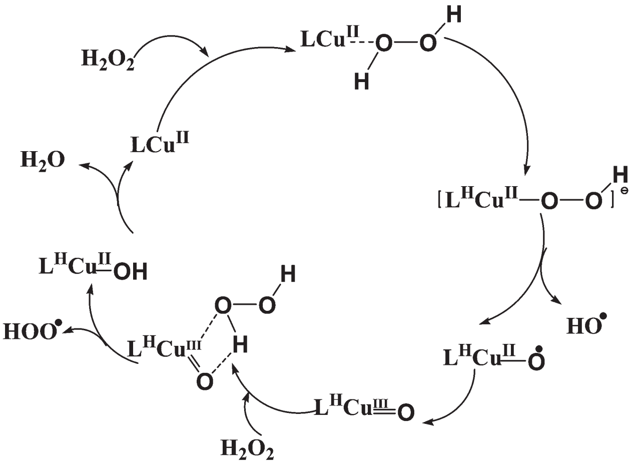

Scheme 3

phenoxo oxygen atom. This proposition is supported from the optimized geometry of $[LCu–OOH]^-$ where the peroxy H atom is strongly H-bonded to the phenoxo oxygen atom of the coordinated ligand. The intermediate L^HCu^{II}–OOH can release one $HO^{\cdot}$ radical with the formation of $L^HCu^{III}{=}O$ which on further steps reacts with another molecule of HOOH leading to the formation of L^HCu^{II}–OH with the concerted release of $HOO^{\cdot}$ radical. L^HCu^{II}–OH releases one water molecule to regenerate the catalyst. Thus in one catalytic cycle two H_2O_2 molecules release one $HO^{\cdot}$ and one $HOO^{\cdot}$ radicals. Thus these radicals could be formed from the metal-assisted decomposition of hydrogen peroxide *i.e.*, through Fenton-like reactions.

The $HO^{\cdot}/HOO^{\cdot}$ radicals abstract H atoms from the substrate (RH) to form $R^{\cdot}$. The formation of ROOH may occur by the reaction between a metal–peroxo intermediate, *e.g.* bearing a Cu(ɪɪ)–OOH type moiety and the organoradical, $R^{\cdot}$ to form ROOH.[59–61] The metal/complex assisted formation of one $HO^{\cdot}$ and one $HOO^{\cdot}$ radicals out of two H_2O_2 has recently been demonstrated by Shul'pin *et al.* through DFT studies.[63] The metal-assisted homolytic cleavage of alkyl hydroperoxide generates alkoxyl ($RO^{\cdot}$, upon O–O bond rupture) and alkylperoxyl ($ROO^{\cdot}$, upon O–H bond fission) radicals which can form an alcohol (ROH) upon H-abstraction from the alkane (RH) by $RO^{\cdot}$ or both ROH and the >C═O upon decomposition of $ROO^{\cdot}$.

Conclusions

Complex **1** has been optimized structurally and the gas-phase data are found to be in good agreement with the X-ray data. It reacts with hydrogen peroxide in presence of a TEA to generate [TEAH][Cu(L)(OOH)] (**2**) which is reasonably stable in solution. DFT calculations reveal that the Cu–O74 (hydroperoxo) bond length is 1.97 Å and is close to the 1.888 Å reported by Masuda and co-workers.[9] The Cu–O74–O75 angle 113° is also in good agreement with the value reported by Masuda (114.5°). It is interesting to note that there is a strong O···H–O–O H-bonding interaction (O2···H76 = 2.27 Å) between phenoxo–O and peroxo H atoms which is shorter than the NH···O(OOH) bond distance (2.78 Å) as found by Masuda and co-workers and believed to be responsible for the stability of hydroperoxo species. These results clearly indicate that a non-covalent interaction is essential for the coordination and stability of small molecules such as HOOH, as predicted by Masuda. The IR spectrum showed a prominent peak at ~880 cm^{-1} and matches reasonably well with the DFT optimized value (896 cm^{-1}) in the gas phase. Thus these hydroperoxo complexes could serve as models for the active center in biological systems such as peptidylglycine α-amidating monooxygenase (PAM) and dopamine β-monooxygenase (DβM) and is evidenced by its catalytic oxidation of toluene with high TON. This reports opens up a new dimension for the stabilization of small molecules such as –OOH coordinated to the metal center through H-bonding in the Schiff-base ligand environment.

Acknowledgements

Financial supports from CSIR (Ref No. 01(2490)/11/EMR-II) and UGC [39-735/2010(SR)], New Delhi, India are gratefully acknowledged.

Notes and references

1 S. Itoh, *Curr. Opin. Chem. Biol.*, 2006, **10**, 115.
2 L. M. Mirica, X. Ottenwaelder and T. D. P. Stack, *Chem. Rev.*, 2004, **104**, 1013.
3 E. A. Lewis and W. B. Tolman, *Chem. Rev.*, 2004, **104**, 1047.
4 J. P. Klinman, *Chem. Rev.*, 1996, **96**, 2541.
5 J. P. Evans, A. Kyunghye and J. P. Klinman, *J. Biol. Chem.*, 2002, **278**, 9691.

6 W. A. Francisco, G. Wille, A. J. Smith, D. J. Merkler and J. P. Klinman, *J. Am. Chem. Soc.*, 2004, **126**, 13168.

7 A. T. Bauman, E. T. Yukl, K. Alkevich, A. L. McCormack and N. J. Blackburn, *J. Biol. Chem.*, 2006, **281**, 4190.

8 P. Chen and E. Solomon, *J. Am. Chem. Soc.*, 2004, **126**, 4991.

9 A. Wada, M. Harata, K. Hasegawa, K. Jitsukawa, H. Masuda, M. Mukai, T. Kitagawa and H. Einaga, *Angew. Chem., Int. Ed.*, 1998, **37**, 798.

10 (*a*) M. Kodera, T. Kita, I. Miura, N. Nakayama, T. Kawata, K. Kano and S. Hirota, *J. Am. Chem. Soc.*, 2001, **123**, 7715; (*b*) P. Chen, K. Fujisawa and E. I. Solomon, *J. Am. Chem. Soc.*, 2000, **122**, 10177; (*c*) T. Fujii, A. Naito, S. Yamaguchi, A. Wada, Y. Funahashi, K. Jitsukawa, S. Nagatomo, T. Kitagawa and H. Masuda, *Chem. Commun.*, 2003, 2700; (*d*) A. Kunishita, M. Kubo, H. Sugimoto, T. Ogura, K. Sato, T. Takui and S. Itoh, *J. Am. Chem. Soc.*, 2009, **131**, 2788.

11 T. Kamachi, Y. M. Lee, T. Nishimi, J. Cho, K. Yoshizawa and W. Nam, *J. Phys. Chem. A*, 2008, **112**, 13102.

12 T. Ohta, T. Tachiyama, K. Yoshizawa, T. Yamabe, T. Uchida and T. Kitagawa, *Inorg. Chem.*, 2000, **39**, 4358.

13 M. Kodera, T. Kita, I. Miura, N. Nakayama, T. Kawata, K. Kano and S. Hirota, *J. Am. Chem. Soc.*, 2001, **123**, 7715.

14 T. Fujii, S. Yamaguchi, Y. Funahashi, T. Ozawa, T. Tosha, T. Kitagawa and H. Masuda, *Chem. Commun.*, 2006, 4428.

15 S. Yamaguchi and H. Masuda, *Sci. Technol. Adv. Mater.*, 2005, **6**, 34.

16 D. Maiti, H. R. Lucas, A. A. N. Sarjeant and K. D. Karlin, *J. Am. Chem. Soc.*, 2007, **129**, 6998.

17 D. Maiti, A. A. N. Sarjeant and K. D. Karlin, *J. Am. Chem. Soc.*, 2007, **129**, 6720.

18 A. Kunishita, J. D. Scanlon, H. Ishimaru, K. Honda, T. Ogura, M. Suzuki, C. J. Cramer and S. Itoh, *Inorg. Chem.*, 2008, **47**, 8222.

19 A. Kunishita, M. Kubo, H. Ishimaru, T. Ogura, H. Sugimoto and S. Itoh, *Inorg. Chem.*, 2008, **47**, 12032.

20 D. Maiti, D. H. Lee, K. Gaoutchenova, C. Würtele, M. C. Holthausen, A. A. N. Sarjeant, J. Sundermeyer, S. Schindler and K. D. Karlin, *Angew. Chem., Int. Ed.*, 2008, **47**, 82.

21 D. Maiti, A. A. N. Sarjeant and K. D. Karlin, *Inorg. Chem.*, 2008, **47**, 8736.

22 L. Q. Hatcher and K. D. Karlin, *Adv. Inorg. Chem.*, 2006, **58**, 131.

23 S. Yamaguchi and H. Masuda, *Sci. Technol. Adv. Mater.*, 2005, **6**, 34.

24 C. Würtele, E. Gaoutchenova, K. Harms, M. C. Holthausen, J. Sundermeyer and S. Schindler, *Angew. Chem., Int. Ed.*, 2006, **45**, 3867.

25 C. Würtele, O. Sander, V. Lutz, T. Waitz, F. Tuczek and S. Schindler, *J. Am. Chem. Soc.*, 2009, **131**, 7544.

26 S. Schindler, *Eur. J. Inorg. Chem.*, 2000, 2311.

27 M. Schatz, M. Becker, O. Walter, G. Liehr and S. Schindler, *Inorg. Chim. Acta*, 2001, **324**, 173.

28 K. Komiyama, H. Furutachi, S. Nagatomo, A. Hashimoto, H. Hayashi, S. Fujinami, M. Suzuki and T. Kitagawa, *Bull. Chem. Soc. Jpn.*, 2004, **77**, 59.

29 D. A. Kunz and P. J. Chapman, *J. Bacteriol.*, 1981, **146**, 179.

30 M. J. Worsey, F. C. H. Franklin and P. A. Williams, *J. Bacteriol.*, 1978, **134**, 757.

31 M. A. Abril, C. Michan, K. N. Timmis and J. L. Ramos, *J. Bacteriol.*, 1989, **171**, 6782.

32 H. Mimoun, L. Saussine, E. Doire, M. Postel, J. Fischer and R. Weiss, *J. Am. Chem. Soc.*, 1983, **105**, 3101.

33 E. Battistel, R. Tassinari, M. Fornaroli and L. Bonoldi, *J. Mol. Catal. A: Chem.*, 2003, **202**, 107.

34 G. B. Shul'pin, G. Süss-Fink and L. S. Shul'pina, *Chem. Commun.*, 2000, 1131.

35 (*a*) J. A. A. W. Elemeans, E. J. A. Bijsterveld, A. E. Rowan and R. J. M. Nolte, *Chem. Commun.*, 2000, 2443; (*b*) R. A. Periana, D. Miranov, D. Taube, G. Bhalla and C. J. Jones, *Science*, 2003, **301**, 814.

36 D. N. Bolon, C. A. Voigt and S. L. Mayo, *Curr. Opin. Chem. Biol.*, 2002, **6**, 125.

37 Y. Lu, S. M. Berry and T. D. Pfister, *Chem. Rev.*, 2001, **101**, 3047.

38 M. Faiella, C. Andreozzi, R. T. M. de Rosales, V. Pavone, O. Maglio, F. Nastri, W. F. DeGrado and A. Lombardi, *Nat. Chem. Biol.*, 2009, **5**, 882.

39 R. L. Koder, J. L. R. Anderson, L. A. Solomon, K. S. Reddy, C. C. Moser and P. L. Dutton, *Nature*, 2009, **458**, 305.

40 A. E. Shilov and G. B. Shul'pin, *Activation and Catalytic Reactions of Saturated Hydrocarbons in the Presence of Metal Complexes*, Kluwer Academic Publishers, Dordrecht, The Netherlands, 2000.

41 M. M. Whittaker, V. L. DeVito, S.A. Asher and J. W. Whittaker, *J. Biol. Chem.*, 1989, **264**, 7104.

42 (*a*) P. A. Frey, *Chem. Rev.*, 1990, **90**, 1343; (*b*) T. T. Harkins and C. B. Grissom, *Science*, 1994, **263**, 958; (*c*) D. Picot, P. J. Loll and R. M. Garavito, *Nature*, 1994, **367**, 243.

43 A. B. Jazdzewski and W. B. Tolman, *Coord. Chem. Rev.*, 2000, **200–202**, 633.

44 E. Tsuchida, H. Nishide and T. Nishiyama, *Macromol. Chem. Phys.*, 1975, **176**(5), 1349.

45 M. Ayala and E. Torres, *Appl. Catal., A*, 2004, **272**, 1.

46 R. L. Lieberman and A. C. Rosenzweig, *Nature*, 2005, **434**, 177.

47 P. Roy, K. Dhara, M. Manassero and P. Banerjee, *Inorg. Chem. Commun.*, 2008, **11**, 265.

48 P. Gamez, P. G. Aubel, W. L. Driessen and J. Reedijk, *Chem. Soc. Rev.*, 2001, **30**, 376.

49 E. Lambert, B. Chabut, S. Chardon-Noblat, A. Deronzier, G. Chottard, A. Bousseksou, J. Tuchagues, J. Laugier, M. Bardet and J. M. Latour, *J. Am. Chem. Soc.*, 1997, **119**, 9424.

50 G. M. Sheldrick, *Acta Crystallogr., Sect. A: Found. Crystallogr.*, 2007, **64**, 112.

51 M. J. Frisch, G. W. Trucks, H. B. Schlegel, G. E. Scuseria, M. A. Robb, J. R. Cheeseman, J. A. Montgomery Jr., T. Vreven, K. N. Kudin, J. C. Burant, J. M. Millam, S. S. Iyengar, J. Tomasi, V. Barone, B. Mennucci, M. Cossi, G. Scalmani, N. Rega, G. A. Petersson, H. Nakatsuji, M. Hada, M. Ehara, K. Toyota, R. Fukuda, J. Hasegawa,

M. Ishida, T. Nakajima, Y. Honda, O. Kitao, H. Nakai, M. Klene, X. Li, J. E. Knox, H. P. Hratchian, J. B. Cross, R. Ammi, C. Pomelli, J. W. Ochterski, P. Y. Ayala, K. Morokuma, G. A. Voth, P. Salvador, J. J. Dannenberg, V. G. Zakrzewski, S. Dapprich, A. D. Daniels, M. C. Strain, O. Farkas, D. K. Malick, A. D. Rabuck, K. Raghavachari, J. B. Foresman, J. V. Ortiz, Q. Cui, A. G. Baboul, S. Clifford, J. Cioslowski, B. B. Stefanov, G. Liu, A. Liashenko, P. Piskorz, I. Komaromi, R. L. Martin, D. J. Fox, T. Keith, A. Al-Laham, C. Y. Peng, A. Nanayakkara, M. Challacombe, P. M. W. Gill, B. Johnson, W. Chen, M. W. Wong, C. Gonzalez and J. A. Pople, *GAUSSIAN 03 (Revision C.02)*, Gaussian, Inc., Wallingford, CT, 2004.

52 A. D. Becke, *J. Chem. Phys.*, 1993, **98**, 5648.

53 P. J. Hay and W. R. Wadt, *J. Chem. Phys.*, 1985, **82**, 299.

54 Y. Yang, M. N. Weaver and K. M. Merz Jr., *J. Phys. Chem. A*, 2009, **113**, 9843.

55 Y. P. Cai, C. Y. Su, A. W. Xu, B. S. Kang, Y. X. Tong, H. Q. Liu and S. Jie, *Polyhedron*, 2001, **20**, 657.

56 T. Tano, M. Z. Ertem, S. Yamaguchi, A. Kunishita, H. Sugimoto, N. Fujieda, T. Ogura, C. J. Cramer and S. Itoh, *Dalton Trans.*, 2011, **40**, 10326.

57 M. Mizuno, K. Honda, J. Cho, H. Furutachi, T. Tosha, T. Matsumoto, S. Fujinami, T. Kitagawa and M. Suzuki, *Angew. Chem., Int. Ed.*, 2006, **45**, 6911.

58 A. M. Kirillov, M. N. Kopylovich, M. V. Kirillova, M. Haukka, M. F. C. Guedes da Silva and A. J. L. Pombeiro, *Angew. Chem., Int. Ed.*, 2005, **44**, 4345.

59 G. S. Mishra and A. J. L. Pombeiro, *J. Mol. Catal. A: Chem.*, 2005, **239**, 96.

60 A. M. Kirillov, M. N. Kopylovich, M. V. Kirillova, E. Yu. Karabach, M. Haukka, M. F. C. G. da Silva and A. J. L. Pombeiro, *Adv. Synth. Catal.*, 2006, **348**, 159.

61 G. B. Shul'pin, G. S. Mishra, L. S. Shul'pina, T. V. Strelkova and A. J. L. Pombeiro, *Catal. Commun.*, 2007, **8**, 1516.

62 P. Roy and M. Manassero, *Dalton Trans.*, 2010, **39**, 1539.

63 M. V. Kirillova, M. L. Kuznetsov, Y. N. Kozlov, L. S. Shul'pina, A. Kitaygorodskiy, A. J. L. Pombeiro and G. B. Shul'pin, *ACS Catal.*, 2011, **1**, 1511.